

# Vortex-antivortex physics in shell-shaped Bose-Einstein condensates

Karmela Padavić,<sup>1,\*</sup> Kuei Sun,<sup>2,†</sup> Courtney Lannert,<sup>3,4,‡</sup> and Smitha Vishveshwara<sup>1,§</sup>

<sup>1</sup>*Department of Physics, University of Illinois at Urbana-Champaign, Urbana, Illinois 61801-3080, USA*

<sup>2</sup>*Department of Physics, The University of Texas at Dallas, Richardson, Texas 75080-3021, USA*

<sup>3</sup>*Department of Physics, Smith College, Northampton, Massachusetts 01063, USA*

<sup>4</sup>*Department of Physics, University of Massachusetts, Amherst, Massachusetts 01003-9300, USA*

Shell-shaped hollow Bose-Einstein condensates (BECs) exhibit behavior distinct from their filled counterparts and have recently attracted attention due to their potential realization in microgravity settings. Here we study distinct features of these hollow structures stemming from vortex physics and the presence of rotation. We focus on a vortex-antivortex pair as the simplest configuration allowed by the constraints on superfluid flow imposed by the closed-surface topology. In the two-dimensional limit of an infinitesimally thin shell BEC, we characterize the long-range attraction between the vortex-antivortex pair and find the critical rotation speed that stabilizes the pair against self-annihilation. In the three-dimensional case, we contrast the bounds on vortex stability with those in the two-dimensional limit and the filled sphere BECs, and evaluate the critical rotation speed as a function of shell thickness. We thus demonstrate that analyzing vortex nucleation provides a non-destructive means of characterizing a hollow sphere BEC and distinguishing it from its filled counterpart.

## I. INTRODUCTION

From the microscopic to the astronomical, shell-shaped Bose-Einstein condensates (BECs) have made their appearance in fascinating ways. In the laboratory realm of ultracold gases, the bosonic optical-lattice setting is renowned for its “wedding-cake” structures [1–5] consisting of Mott-insulating layers sandwiching superfluid shells, while other instances of such shells include Bose-Fermi mixtures [6–8]. In the stellar realm, extremely high densities in neutron stars offer the possibility of hosting condensed phases of subatomic particles, and some observed behavior has indicated shell-shaped superfluid regions [9–11]. BEC shells are expected to have dramatically different features from their filled counterparts in collective mode structure [12–14], thermodynamics [15, 16], and time-of-flight properties [17–19]. A proposed “bubble trap” geometry [20] in laboratory settings would allow for the realization of BEC shells in free space and the controlled tuning from a filled sphere to a topologically distinct [12, 13] hollowed out three-dimensional (3D) structure to a two-dimensional (2D) spherical surface. While so far gravitational sag has prevented the creation and analysis of free standing hollow shells on Earth, the advent of experiments in microgravity [21, 22] holds promise. In particular, one experiment in the recently launched Cold Atomic Laboratory (CAL) aboard the International Space Station specifically designed to realize a hollow bubble geometry [23, 24], has provided impetus for probing the unique topological and geometric aspects of BEC shells.

Integral to BECs, the physics of quantized vortices [25] in shell-shaped structures calls for a study in and of itself. In tuning through the dimensional crossover from a filled sphere to a thin shell, a single vortex line passing through the filled system reduces a vortex-antivortex pair on the 2D shell surface. The associated thermodynamics is highly sensitive to the closed geometry and topology, particularly with regards to vortex-antivortex induced Berezinskii-Kosterlitz-Thouless transition [26]. In the presence of stirring or rotation, static and dynamic features of vortices in shell BECs are expected to be significantly altered compared to filled sphere counterparts. An extreme instance involves possible explanations for pulsar glitches attributed to tangles of vortices in neutron stars [11]. Here, we demonstrate that even the simplest vortex configuration in a spherical shell geometry exhibits rich physics due to interplay between restricted flow in a closed topology and the energetics of vortices in hollow structures. Topological constraints enforce a zero circulation rule, applicable even to classical fluids such as planetary atmospheres [27], requiring that the vortex-antivortex pair be the minimally allowed configuration [28, 29], in contrast to a flat 2D system where a single isolated vortex is possible. We investigate equilibrium properties of such a pair across the finite thickness to strictly 2D shell regimes, establishing that upon rotation they are stable only when at the poles. The energy barrier for nucleating such a pair in a shell always remains less than for a filled sphere of the same radius, as expected from the absence of core energy in the hollow region. Along with previous predictions for collective mode excitations in BEC shells [12, 13], these studies provide a non-destructive means for characterizing a hollow sphere and distinguishing it from its filled counterpart.

Our starting point for analyzing vortex structures in shell-shaped BECs assumes a condensate wavefunction  $\psi = f e^{iS}$ , where  $S$  represents the condensate wavefunction phase and  $f$  its amplitude. For the 2D and 3D

\* kpadavi2@illinois.edu

† kuei.sun@utdallas.edu

‡ clannert@smith.edu

§ smivish@illinois.edu

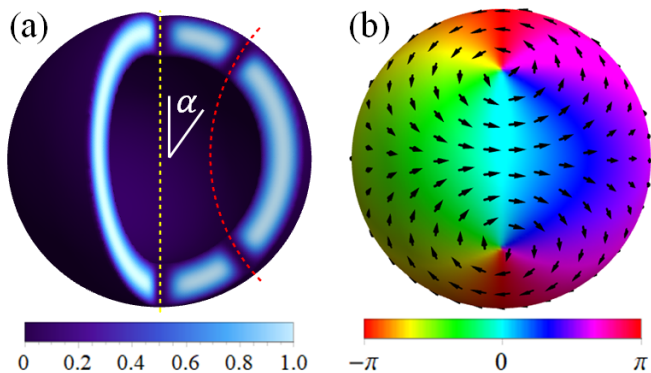


FIG. 1. (a) A schematic density profile of a shell-shaped BEC comparing a vortex-antivortex pair at the poles, rotating about the  $z$  axis (straight dashed line) with another such pair at polar angle  $\theta = \alpha$  (antivortex at  $\pi - \alpha$ ) rotating about a curved dashed line. (b) Vector field showing superfluid flow for the vortex-antivortex pair at  $\theta = \alpha$ . The  $+x$  direction points out of page, and the colors represent the phase  $S$  of the BEC wavefunction.

cases,  $f$  is related to the condensate density  $f^2 = \rho_{2D}$  or  $\rho$ , respectively. The condensate velocity takes the form  $v = \hbar \nabla S / m$  for condensate atoms of mass  $m$ . Near the vortex center, the rotation speed of condensate atoms exceeds the Landau criterion for destruction of superfluidity and a vortex “core” is formed. The size of this density depletion is set by the condensate’s healing length  $\xi_0$ , which depends on the strength of interatomic interactions.

In what follows, we first consider a 2D BEC confined to the surface of a sphere, detailing the topological constraints on and interactions between vortices in this closed, curved geometry. We find that long-range attractive interactions tend to cause a vortex-antivortex pair to annihilate, while rotation of the system tends to drive them to opposite poles. Within a Gross-Pitaevskii (GP) formalism that allows us to include the interactions between condensate atoms and the nonzero size of the vortex cores, we find the critical rotation speed necessary to stabilize the pair. We chart the condensate flow pattern in the presence of the associated vortex line threading through the 2D surface system, as shown in Fig. 1(a). Turning to thin 3D hollow shells, we use a simple slicing argument and a local density approximation to argue that a critical rotation speed for nucleating a single vortex line persists in this more realistic curved hollow system and show that its value increases with the thickness of the shell. We perform a fully 3D numerical solution of the GP equation in order to obtain estimates of the critical rotation speed for a hollow shell away from the thin-shell limit and compare it to the case of a filled sphere. We conclude with a brief outlook on dynamics and multi-vortex scenarios in the context of BEC shells.

## II. VORTICES ON A TWO-DIMENSIONAL SPHERICAL SURFACE

While the precise distribution of vortices and superfluid flow patterns for a hollow condensate shell depends on its geometry and detailed energetics, the  $S^2$  topology associated with the closed surface poses significant constraints [30]. By way of illustration, we first discuss an infinitesimally thin, effectively 2D shell BEC. Consider a collection of  $n_v$  point-like vortices on the surface of the sphere having integer vorticities  $\ell_i$ , respectively. Units of circulation within any closed loop on the surface can be counted using a loop integral, equivalent to a surface integral via Stokes’ theorem ( $\oint \nabla S \cdot dl = \oint \frac{\hbar}{m} v \cdot dl$ ). If the loop is chosen to contain all vortices, then the rest of the shell contains no vortices and we identify the constraint of vanishing net vortex circulation,  $\sum_{i=1}^{n_v} \ell_i = 0$ . Such constraints have been identified for a broader class of compact surfaces, for instance toroidal surfaces of revolution in Ref. [30]. The simplest instance of vortex nucleation on the surface of a spherically symmetric BEC, the focus of this work, then is  $n_v = 2$  and  $\ell_1 = -\ell_2 = 1$  [28, 29]. This describes a vortex carrying a single unit of angular momentum in tandem with an identical vortex having the same vorticity but oriented in the opposite direction, i.e. a vortex-antivortex pair.

Further, a non-zero flow field on the condensate shell has to satisfy the Poincaré-Hopf theorem, which states that for a vector field everywhere tangent to the surface of a sphere, the topological indices associated with its zeroes and singularities must add up to its Euler characteristic. This theorem is equally applicable to fluid flow in other settings, such as the Earth’s atmosphere [27]. Explicitly, denoting a topological charge of the  $i$ th defect in a collection of  $n_d$  vortices and singular flow points on the surface of a sphere as  $q_i$  implies  $\sum_{i=1}^{n_d} q_i = 2$ . Regardless of its vorticity,  $\ell_i$ , a point vortex here has topological charge  $q_i = 1$ , while stagnation points in the flow contribute  $q_i = -1$ . The vortex-antivortex pair ( $q_i = 1$  each) in the absence of any stagnation points in the superfluid flow is thus the simplest allowed vortex configuration for the condensate shell under the constraints posed by its geometry and topology.

Two point-like vortices carrying opposite vorticities in a 2D condensate experience an attractive interaction. Intuitively, interactions between vortices stem from their being sources of vorticity for the superfluid flow—as the superfluid circulates around each vortex, this motion carries other vortices with it. In this sense, vortex interaction energy reflects the kinetic energy of the underlying condensate. Similar physics occurs for a collection of current carrying wires where each wire is affected by a Lorentz force due to magnetic fields produced by other wires [31]. To make the superfluid vortex case more precise, as in Refs. [32, 33], we write this effective flow-mediated interaction energy as

$$E_{v-v} = \frac{\hbar^2 \rho_{2D}}{2m^2} \int |\nabla S|^2 dA \quad (1)$$

and calculate this energy using a Green's function method.

For a vortex-antivortex pair situated at  $(\theta, \phi) = (\alpha, 0)$  and  $(\pi - \alpha, 0)$ , respectively (see examples in Fig. 1) i.e. a dipole-like configuration symmetric about the equator of the BEC shell, this interaction energy takes the form

$$E_{v-av}(\alpha) = \frac{\pi \hbar^2 \rho_{2D}}{m^2} \ln(\cos \alpha). \quad (2)$$

Here, the shell topology is reflected in the logarithmic scaling of interaction energy with the angular separation of vortices, rather than with the rectilinear distance between them, which is the case in flat superfluid topologies. For the vortex-antivortex pair, the condensate kinetic energy decreases as  $\alpha \rightarrow \pi/2$ , resulting in an attractive interaction. In the full  $\alpha = \pi/2$  limit, the vortices overlap and annihilate at the equator and the flow sourced by either, and its associated kinetic energy, vanishes. A vortex-antivortex pair in a flat 2D superfluid experiences a similar attraction [34, 35].

Given this attractive interaction, we investigate whether external rotation of the system can stabilize the pair against annihilation. For a rotating system, the total energy of vortices decreases as the system's angular momentum increases. Since angular momentum is maximized when the two vortices align with the rotation axis, we expect a minimum of the total vortex energy for  $\alpha = 0$  and sufficiently fast shell rotation. Heuristically, transforming the shell energy to a rotating frame with angular velocity  $\Omega$ ,  $E \rightarrow E - \Omega \langle L_z \rangle$  implies the same conclusion.

To formalize this intuitive understanding that condensate flow on the 2D shell pulls vortices having opposite circulations closer together, but rotation pushes them apart and towards the rotation axis, we evaluate the energy associated with rotation to be

$$E_{\text{rot}} = \Omega \langle L_z \rangle = 4\pi \frac{\hbar}{m} \rho_{2D} \Omega R^2 \cos \alpha. \quad (3)$$

Here,  $R$  is the shell radius, and  $R^2 \cos \alpha$  indicates that rotational energy scales as the surface area covered by the condensate atoms set in motion by each vortex. Combining Eqs. (2) and (3), the dimensionless form of the energy per particle in the rotating frame becomes

$$\varepsilon(\alpha) = \frac{E_{v-av} - E_{\text{rot}}}{NE_R} = \frac{1}{2} \ln(\cos \alpha) - \tilde{\Omega} \cos \alpha, \quad (4)$$

where  $N = 4\pi R^2 \rho_{2D}$  is the total number of condensed atoms,  $E_R = \hbar^2/(2mR^2)$  sets the characteristic energy scale, and  $\tilde{\Omega} = \frac{2m}{\hbar} \Omega R^2$  is a dimensionless angular velocity.

Based on this energetic form, Fig. 2(a) shows that the energy functional exhibits differing behaviors for  $\tilde{\Omega}$  above or below a critical value  $\tilde{\Omega}_c = \frac{1}{2}$ . The global minimum of  $\varepsilon(\alpha)$  is always at  $\alpha = \frac{\pi}{2}$ . If  $\tilde{\Omega} \leq \tilde{\Omega}_c$ ,  $\varepsilon(\alpha)$  monotonically decreases with  $\alpha$ , again implying the tendency towards self-annihilation of the pair at  $\alpha = \frac{\pi}{2}$ . If  $\tilde{\Omega} > \tilde{\Omega}_c$ ,  $\varepsilon(\alpha)$  develops a local minimum at  $\alpha = 0$  and a local

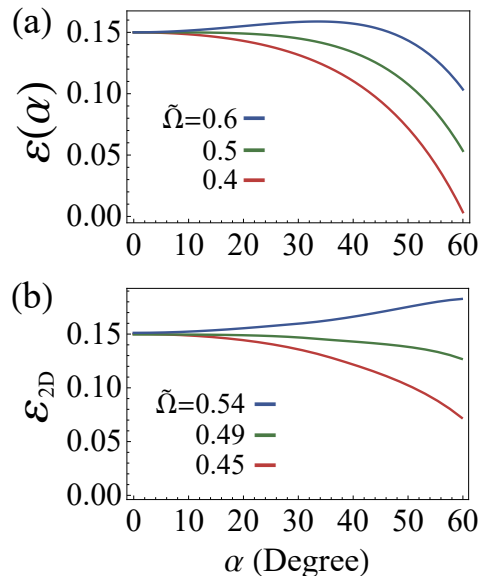


FIG. 2. (a) Dimensionless superfluid flow-based energy  $\varepsilon(\alpha)$  [in Eq. (4)] of a rotating 2D spherical BEC for dimensionless angular velocity  $\tilde{\Omega}$  for values that are i) above, ii) equal to, and iii) below the critical value  $\tilde{\Omega}_c = \frac{1}{2}$  where a local minimum develops for a polar vortex-antivortex pair. (b) Dimensionless energy  $\varepsilon_{2D}$  [in Eq. (5)] obtained from the numerical GP calculations. For ease of comparison, we have shifted energy curve offsets so as to align at  $\alpha = 0$ . The dimensionless energies are in units of the characteristic energy  $E_R = \hbar^2/(2mR^2)$ , where  $R$  is the spherical radius.

maximum at  $\alpha = \alpha_M = \cos^{-1}(1/2\tilde{\Omega})$ , decreasing for  $\alpha_M < \alpha < \frac{\pi}{2}$ . Any vortex-antivortex pair initially located at  $0 < \alpha < \alpha_M$  tends to nucleate along the rotation axis, while for  $\alpha > \alpha_M$  the pair is unstable to self-annihilation at  $\alpha = \frac{\pi}{2}$  (the shell's equator) regardless of system rotation. However, for angles near  $\alpha = \frac{\pi}{2}$ , we may no longer disregard vortex core effects, and this energy functional no longer holds.

To complete our analysis of the 2D vortex-antivortex pair energetics, we next include the effects of actual interactions between the atoms in the BEC. This also implies that we consider vortices as having density depletion at their cores over the size of the healing length  $\xi_0$  set by the strength of these interactions instead of being point-like. We numerically calculate the wavefunction  $\psi_{2D}(\theta, \phi)$  of a rotating 2D spherical BEC by minimizing the energy functional in the rotating frame (the standard GP formalism),

$$\varepsilon_{2D}[\psi_{2D}] = \int \sin \theta d\theta d\phi [|\nabla \psi_{2D}|^2 + \frac{U_{2D}}{2} |\psi_{2D}|^4 + \tilde{\Omega} \psi_{2D}^* (i\partial_\phi) \psi_{2D}], \quad (5)$$

which is rendered dimensionless by  $E_R$ . Here,  $U_{2D}$  is the dimensionless 2D effective interaction strength, which is set to keep the typical ratio of kinetic energy to interaction energy to be  $\sim 5\%$  (e.g.,  $U_{2D} = 1000$  in our simu-

lation). The vortex-antivortex pair configuration is imposed by fixing the wavefunction zeros (vortex cores) at  $\alpha$  and  $\pi - \alpha$ . In Fig. 2(b), we plot the energy functional obtained by this GP calculation. The curves exhibit behavior above and below a critical angular velocity  $\tilde{\Omega}_c \sim \frac{1}{2}$  consistent with Fig. 2(a), confirming the stability of the vortex-antivortex pair at the condensate shell poles for sufficiently fast rotation. Numerical results in Fig. 2(b) also show the energy functional's decrease toward the global minimum at  $\alpha = \pi/2$  to be less drastic than suggested by the analytic results in Fig. 2(a) [Eq. (4)]. This reflects the effect of density depletion at the vortex cores moderating the inter-vortex interaction at close separations.

Focusing on the superfluid flow obtained from the GP wavefunction, for any finite  $\alpha$  we find that the flow pattern resembles one that rotates about a string through both vortex cores, as illustrated in Fig. 1. We employ a variational approach to approximate the wavefunction by considering the shape of such a string, parameterized in a convenient way. This allows us to determine the condensate density and phase, and the associated superfluid flow. We set an arbitrary conic-section curve on the  $x$ - $z$  plane ( $\phi = 0$  or  $\pi$ ) through the vortex cores on the sphere which takes the general form  $z^2 = (\lambda - 1)x^2 + 2bx + (1 - \lambda \sin^2 \alpha - 2b \sin \alpha)$  with two variational parameters  $b$  and  $\lambda$ . We numerically minimize the energy functional of Eq. (5) with a variational wavefunction  $\psi_{\text{var}}(\theta, \phi) = f_{\text{var}} e^{iS_{\text{var}}}$ , where the phase  $S_{\text{var}}$  is now the azimuthal angle with respect to the variational curve, and the amplitude  $f_{\text{var}}$  has a variational depletion at the vortex cores. Specifically,  $f_{\text{var}}(\theta, \phi) = A \frac{\sigma_\alpha}{\sqrt{\zeta^2 + \sigma_\alpha^2}} \times \frac{\sigma_{\pi-\alpha}}{\sqrt{\zeta^2 + \sigma_{\pi-\alpha}^2}}$ , where  $A$  is the normalization constant,  $\zeta$  a variational parameter, and  $\sigma_\alpha = \cos^{-1}(\cos \alpha \cos \theta + \sin \alpha \sin \theta \cos \phi)$  is the distance from the vortex core at  $\alpha$ . We find that the minimum energy state corresponds to a circle string ( $\lambda = 1$ ) passing through the vortex cores and perpendicular to the sphere's surface. Further, these variational results qualitatively agree with the GP results with respect to energy functional curves as well as critical rotation speed.

The variational assumption of a curved string connecting the vortex-antivortex pair relates our analysis to studies of vortex dynamics in filled 3D spherical BECs where a physical vortex string (line) may move off-axis [36, 37] or bend [38–40] due to interaction or density inhomogeneity effects. Namely, a vortex-antivortex pair on opposite poles of a 2D condensate shell corresponds to a straight on-axis vortex in a 3D BEC, while the pair at angle  $\alpha > 0$  corresponds to a bent vortex. This correspondence additionally informs the understanding of vortices on a spherically symmetric BEC undergoing dimensional crossover from a hollow 2D geometry to a shell-shaped condensate having finite thickness and, finally, to a fully filled spherical BEC. Such crossover could be experimentally achieved by the bubble trap [20] which we model in the next sections of this work.

The 2D condensate shell, as we have shown so far,

captures rich physics in and of itself. Here, flow-based attractive vortex-vortex interactions cause the simplest vortex arrangement allowed by the shell-shape — the vortex-antivortex pair — to annihilate in the absence of rotation. Vortices can be stabilized against annihilation by rotating the system above some critical rotation speed and, with the view of dimensional crossover, the same stabilization would occur for an equivalent single vortex line along the rotation axis in a condensate shell away from the truly 2D limit. Interatomic interactions within the condensate, and consequent non-zero vortex core size, further lessen the attractive interaction between the vortex-antivortex pair at short inter-vortex separations.

### III. THIN THREE-DIMENSIONAL SHELLS

Expanding on our observations in the 2D limit, we analyze the realistic case of a thin but not perfectly 2D spherical condensate shell containing a vortex line (the natural extension of the 2D shell vortex-antivortex pair) from multiple perspectives. First, using a Thomas-Fermi (TF) approximation, we compare the energetics in the thin shell with that in the case of a filled shell. We next approach the thin shell from the 2D limit by building up the former as several layers of latter. Finally, we use the 3D GP energy functional analogous to Eq. (5) [36] and include a bubble trapping potential to rigorously corroborate the comparison and obtain accurate estimates for critical rotation frequencies.

To estimate the energy cost of a vortex line in a shell-shaped condensate and compare with a filled sphere, we closely follow the approach for the latter in Ref. [36], which is expected to be valid in the TF limit i.e when the condensate healing length is small compared to its radius (or thickness). The situation considered here, a single vortex line along the  $z$  axis having winding  $\ell$ , can be described by the BEC wavefunction  $\psi(\mathbf{r}) = f(r_\perp, \theta) e^{i\ell\phi}$  (in cylindrical polar coordinates). Assuming an  $\ell = 1$  vortex, we imagine slicing the condensate (either filled sphere or hollow shell) into thin sections of height  $dz$ , then integrating over  $z$ . For a harmonically confined system (filled-sphere BEC) where each slice is a disk BEC pierced through its center by the vortex core, Ref. [36] finds the fractional energy cost of the vortex to be

$$E_{\text{vortex}}^{\text{sphere}}/E_{\text{sphere}} \approx \frac{4\pi\hbar^2}{3mU} R \left( \ln \frac{R}{\xi_0} - 0.399 \right). \quad (6)$$

Here,  $U$  is the 3D interatomic interaction strength,  $\xi_0$  is the coherence length at the center of the vortex-free BEC, and  $R$  is its outer radius. We note that the vortex core size is set by  $\xi_0$ , which should be much smaller than the size of the cloud,  $R/\xi_0 \gg 1$ .

For a thin spherical shell having thickness  $\delta$ , much smaller than outer radius  $R$ , a similar slicing procedure now includes two disks (at the top and bottom of the system) and a number of intervening thin annuli, all with

the vortex threading through their centers, perpendicular to the slicing plane. The resulting fractional energy cost of the vortex in this system is:

$$E_{\text{vortex}}^{\text{thinshell}}/E_{\text{thinshell}} \approx \frac{2\pi\hbar^2}{3mU}\delta \left( \ln \frac{R}{\xi_0} + \ln \frac{\delta}{\xi_0} + 4.597 \right), \quad (7)$$

where  $\xi_0$  is the coherence length at the mean radius of the shell and we note that, as above for the sphere, we assume  $\delta/\xi_0 \gg 1$ . We note that since  $R \gg \delta$  for a thin shell, the first term in parentheses dominates.

Based on this analytical calculation we conclude that the energy cost of a vortex in a thin shell BEC scales linearly with its thickness. In contrast, the energy cost of a vortex in a filled sphere BEC scales linearly (with log corrections) with its radius  $R$ . This result suggests that the dominant cost of a vortex is its core, which has length  $2R$  in the filled sphere and only  $2\delta$  for the thin shell. Since in the thin shell limit we assume a hollow BEC thickness much smaller than its radius, the energy cost for a vortex in this geometry will be much lower than for a similarly sized fully filled spherical condensate.

Having compared the hollow shell with the filled sphere, we now turn to the opposite limit of using a local density approximation (LDA) to decompose a thin 3D shell into layers of concentric 2D shells with radii ranging between the 3D BEC's inner Thomas-Fermi radius  $R_{\text{in}} = R - \delta$  and its outer Thomas-Fermi radius  $R$ . Within this approach, a vortex line in the 3D condensate shell (spanning its thickness) is equivalent to a stack of 2D vortices, each associated with one concentric shell layer. The system's energy functional is evaluated as

$$\varepsilon_{3\text{D}}^{\text{LDA}} = \sum_i \varepsilon_{2\text{D}}(r_i). \quad (8)$$

Here,  $\varepsilon_{2\text{D}}(r_i)$  is the energy of each 2D layer, taking the same form as Eq. (5) except with the layer radius equal to  $r_i$ . The effective rotation speed for each 2D layer is scaled here by its radius as  $\tilde{\Omega}^{\text{LDA}}(r_i) = (r_i^2/R^2)\tilde{\Omega}$ , thus contributing an  $r$ -dependent rotational energy to the total energy functional. Therefore, there ought to exist a radius  $r_c$ , such that the effective rotation speed is large enough to stabilize a vortex pair on the poles for the layers with  $r_i > r_c$  (the 'outer' layers) but not for those with  $r_i < r_c$  (the 'inner' layers). Since the vortex line cannot break into parts, its stability is determined by the layers that energetically dominate and thus depends on both the rotation speed  $\tilde{\Omega}$  (which determines  $r_c$ ) and the shell thickness  $\delta$  (which determines the relative energetic contributions between the outer and inner layers).

Given a fixed rotation speed, the thicker the shell, the more the inner layers contribute to the system's energy. Thus, we expect to identify a critical thickness beyond which the local energy minimum for a vortex line piercing through the poles disappears. Figure 3(a) shows the energy functional of shell BECs having various thicknesses at  $\tilde{\Omega} = 0.6$  (with the vortex location fixed at  $\theta = \alpha$  on each 2D layer). The critical thickness above which the

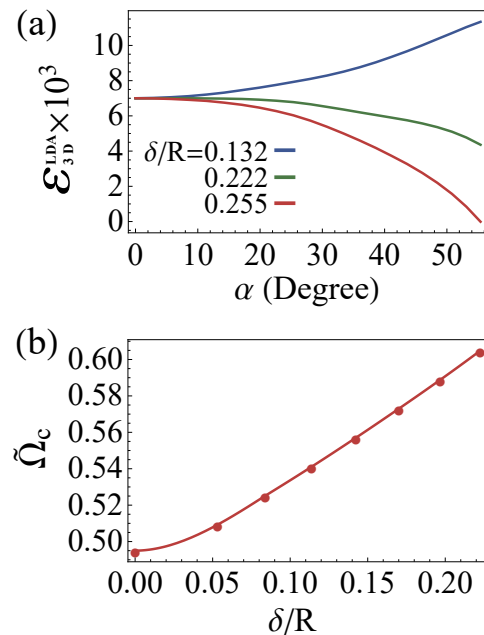


FIG. 3. (a) Dimensionless energy  $\varepsilon_{3\text{D}}^{\text{LDA}}$  [in Eq. (8)] of 3D shell BECs as a function of vortex location for various shell thickness  $\delta$  and dimensionless rotation speed  $\tilde{\Omega} = 0.6$ . The data are from the LDA calculation and are off-set to level up at the  $\alpha = 0$  point. (b) Critical rotation speed  $\tilde{\Omega}_c$  versus shell thickness from the LDA calculation. The leftmost data point is for a pure 2D shell.

vortex line is no longer stable at the poles in this case corresponds to  $\delta/R = 0.222$ .

Conversely, for a given thickness, the LDA calculations show a critical rotation speed that determines the stability of the vortex line through the poles. In Fig. 3(b), we plot the critical rotation speed as function of BEC shell thickness, and find an approximately linear relationship. This result suggests a non-destructive way to experimentally probe the thickness of a BEC shell by finding the lowest rotation speed that stabilizes a single vortex aligned with the rotation axis and passing through the poles.

In using the LDA above, we ignore any possible coupling between the 2D layers. This includes inter-layer particle movements that would result in a radial superfluid current and associated kinetic energy. For a rotating 3D shell BEC having thickness similar to the critical value (at that rotation rate), we expect a very flat energy functional indicating an approximate tie in the competition between outer and inner layers. In such a case, the radial energy, mostly coming from the tilting or bending of the vortex line, might play a significant role in vortex stability. However, for thin enough shells, we do not expect these effects to be important; for thin condensate shells, effects beyond the LDA should not qualitatively change the vortex behavior found in the LDA calculations.

To generalize our discussion further and address the

limitations of not only the Thomas-Fermi but also the LDA, we turn to a numerical solution of the 3D GP equation with a vortex having vorticity  $\ell$  along the  $z$  axis. The resulting energy equation for the condensate wavefunction magnitude,  $f$ , can be minimized using an imaginary-time algorithm [41]. By taking the confining potential to be a bubble trap, we can numerically solve for the ground state wavefunction amplitude and energy for a harmonically trapped filled spherical condensate, as well as a hollow BEC shell. The choice of the bubble trap, in particular, makes this calculation relevant for a large class of spherically symmetric condensates of arbitrary size, hollowness and thickness.

In order to compare with our calculations above, we report results on a fairly thin shell with thickness-to-radius ratio  $\delta/R \approx 0.3$  and confinement frequency  $\omega_0$ . We compare these results to the case of a filled sphere BEC trapped with the same confinement frequency. In order to compare with the Thomas-Fermi results we presented thus far, we work with a relatively large interaction strength: for the spherical and shell systems described above, without a vortex imposed, the ratio of kinetic to interaction energy in the ground state varies through the range 2-20% (from the filled sphere to the thin shell).

By numerically obtaining the ground state energy for the no-vortex ( $\ell = 0$ ) and single-vortex ( $\ell = 1$ ) cases, we obtain the critical rotation for nucleation of a vortex. For the thin ( $\delta/R \approx 0.3$ ) shell, we find  $\Omega_c = 0.02\omega_0$ , whereas for the filled sphere we find  $\Omega_c = 0.2\omega_0$ . This factor of ten difference in critical rotation speeds bears out and illustrates the much lower energy cost for a vortex in a hollow shell, compared with a filled sphere, in accordance with our previous discussions. Recent experiments aboard the Cold Atom Lab [23] working to create a hollow shell-shaped condensate have estimated confinement frequencies of 100-1000 Hz, giving a predicted critical rotation speed of 2-20 Hz from both the simple slicing argument in Eq. (7) and the imaginary time numerical calculations for the BEC shell.

To consolidate our findings for thin shells and their implications, in considering a straight vortex line connecting the poles of a spherically symmetric condensate, we always expect a much smaller energy cost for this vortex configuration in a hollow BEC than in a filled one based on comparing the length of the vortex core in the two systems. We have shown this to be the case through a simple slicing argument and a more general numerical method. We therefore expect that vortices will be much easier to nucleate in a hollow shell system than in a filled system of the same outer shape. Consequently, as with flat nearly 2D BEC layers compared to more 3D bulk structures, the spontaneous appearance of vortices in a hollow system should happen at a lower temperature than for a filled system. This is a reflection of the Berezinskii-Kosterlitz-Thouless superfluid transition temperature [26] being lower than the BEC transition temperature in two dimensions.

Using a LDA and a fully 3D numerical method, we have further shown that there is a critical rotation speed necessary to stabilize a vortex line along the rotation axis and that this critical rotation speed is much smaller for a hollow shell BEC than for a filled-sphere condensate of the same number of particles. Since a vortex-antivortex pair on opposite poles of a 2D condensate shell has a 3D counterpart in the vortex line extending along the rotation axis, this result highlights the validity of our reasoning across hollow BECs of differing dimensionality. Finally, we note that as the LDA results show that a local minimum develops at  $\alpha = 0$  (and at no non-zero angle) at the critical rotation frequency, the hollowness of a system could be probed experimentally by looking for vortex nucleation as a function of rotation or stirring speed.

#### IV. OUTLOOK/FUTURE WORK

While our focus has been on vortex nucleation and equilibrium features, dynamic considerations may be crucial and complex, as found in fully filled condensates. In these cases, off-axis vortex lines are unstable even in spherical geometries in the presence of dissipation which serves to move the vortex line from a local to a global minimum [36]. They tend to precess in radially symmetric 2D geometries [42] and bend in cigar-shaped condensates [38–40]. We note that the “slicing and stacking” method used above, combined with these dynamical results, would imply that a vortex line nucleated at a lateral off-set from the rotation axis in a thin condensate shell would be unstable to bending or dissipation-driven motion towards the outer edge of the condensate [43]. This can be validated using the method of images to show that a point vortex in a 2D annular BEC has a non-zero velocity depending on condensate radii [43, 44]. However, high condensate rotation speed could stabilize a vortex line against bending or excitations (for instance Kelvin waves [45, 46]) through angular momentum effects similar to those discussed above. Various experiments in related contexts hint at this behavior, such as in Ref. [37], where a vortex line in a prolate harmonically trapped BEC becomes more bent and deviates more from the center of the condensate as the angular momentum of the system decreases.

Furthermore, many BEC situations of physical relevance are likely to involve complex multi-vortex dynamics. Vortices are often nucleated as a consequence of perturbing condensates; the dynamical instability of vortex lines presents a starting point for understanding subsequent re-equilibration processes. In systems with fast rotation, equilibrium and dynamic behavior induces a range of structures, including vortex lattices [47–49], giant vortices [50], and tangles of vortex lines. In the context of BEC shells too, we expect diverse dynamic and multi-vortex phenomena that are modified in comparison with their filled counterparts due to the different ge-

ometry and topology. We have shown this to be the case for the vortex-antivortex pair, which in principle could be systematically investigated in the CAL experiment in the future. Our study also offers a first step towards deconstructing theoretical and experimental multi-vortex dynamic studies in a range of settings from CAL and other ultracold atomic systems to pulsar glitches observed in the context of neutron stars [11].

## ACKNOWLEDGMENTS

We thank Nathan Lundblad for illuminating discussions. KP, SV, and CL acknowledge support by NASA (SUB JPL 1553869 and 1553885). SV thanks UC San Diego for its hospitality through the Burbidge Visiting Professorship program.

- 
- [1] G. G. Batrouni, V. Rousseau, R. T. Scalettar, M. Rigol, A. Muramatsu, P. J. H. Denteneer, and M. Troyer, “Mott domains of bosons confined on optical lattices,” *Phys. Rev. Lett.* **89**, 117203 (2002).
- [2] B. DeMarco, C. Lannert, S. Vishveshwara, and T.-C. Wei, “Structure and stability of mott-insulator shells of bosons trapped in an optical lattice,” *Phys. Rev. A* **71**, 063601 (2005).
- [3] Gretchen K. Campbell, Jongchul Mun, Micah Boyd, Patrick Medley, Aaron E. Leanhardt, Luis G. Marcassa, David E. Pritchard, and Wolfgang Ketterle, “Imaging the mott insulator shells by using atomic clock shifts,” *Science* **313**, 649 (2006).
- [4] R. A. Barankov, C. Lannert, and S. Vishveshwara, “Coexistence of superfluid and mott phases of lattice bosons,” *Phys. Rev. A* **75**, 063622 (2007).
- [5] Kuei Sun, Courtney Lannert, and Smitha Vishveshwara, “Probing condensate order in deep optical lattices,” *Phys. Rev. A* **79**, 043422 (2009).
- [6] Klaus Mølmer, “Bose condensates and fermi gases at zero temperature,” *Phys. Rev. Lett.* **80**, 1804 (1998).
- [7] S. Ospelkaus, C. Ospelkaus, L. Humbert, K. Sengstock, and K. Bongs, “Tuning of heteronuclear interactions in a degenerate fermi-bose mixture,” *Phys. Rev. Lett.* **97**, 120403 (2006).
- [8] Bert Van Schaeybroeck and Achilleas Lazarides, “Trapped phase-segregated bose-fermi mixtures and their collective excitations,” *Phys. Rev. A* **79**, 033618 (2009).
- [9] F. Weber, “Strange quark matter and compact stars,” *Progress in Particle and Nuclear Physics* **54**, 193 (2005).
- [10] C. J. Pethick, Thomas Schaefer, and A. Schwenk, “Bose-einstein condensates in neutron stars,” (2015), [arXiv:1507.05839](https://arxiv.org/abs/1507.05839).
- [11] V. Khomenko and B. Haskell, “Modelling pulsar glitches: The hydrodynamics of superfluid vortex avalanches in neutron stars,” *Publications of the Astronomical Society of Australia* **35**, E020 (2018).
- [12] Karmela Padavić, Kuei Sun, Courtney Lannert, and Smitha Vishveshwara, “Physics of hollow bose-einstein condensates,” *EPL (Europhysics Letters)* **120**, 20004 (2017).
- [13] Kuei Sun, Karmela Padavić, Frances Yang, Smitha Vishveshwara, and Courtney Lannert, “Static and dynamic properties of shell-shaped condensates,” *Phys. Rev. A* **98**, 013609 (2018).
- [14] Pedro C. Diniz, Eduardo A. B. Oliveira, Aristeu R. P. Lima, and Emanuel A. L. Henn, “Ground state and collective excitations of a dipolar bose-einstein condensate in a bubble trap,” *Scientific Reports* **10**, 4831 (2020).
- [15] A. Tononi and L. Salasnich, “Bose-einstein condensation on the surface of a sphere,” *Phys. Rev. Lett.* **123**, 160403 (2019).
- [16] Slvio Jacob Bereta, Lucas Madeira, Vanderlei S. Bagnato, and Mnica A. Caracanhas, “Boseeinstein condensation in spherically symmetric traps,” *American Journal of Physics* **87**, 924 (2019).
- [17] C. Lannert, T.-C. Wei, and S. Vishveshwara, “Dynamics of condensate shells: Collective modes and expansion,” *Phys. Rev. A* **75**, 013611 (2007).
- [18] A. Tononi, F. Cinti, and L. Salasnich, “Quantum bubbles in microgravity,” (2019), [arXiv:1912.07297](https://arxiv.org/abs/1912.07297).
- [19] Matthias Meister, Albert Roura, Ernst M Rasel, and Wolfgang P Schleich, “The space atom laser: an isotropic source for ultra-cold atoms in microgravity,” *New Journal of Physics* **21**, 013039 (2019).
- [20] O. Zobay and B. M. Garraway, “Two-dimensional atom trapping in field-induced adiabatic potentials,” *Phys. Rev. Lett.* **86**, 1195 (2001).
- [21] T. van Zoest, N. Gaaloul, Y. Singh, H. Ahlers, W. Herr, S. T. Seidel, W. Ertmer, E. Rasel, M. Eckart, E. Kajari, S. Arnold, G. Nandi, W. P. Schleich, R. Walser, A. Vogel, K. Sengstock, K. Bongs, W. Lewoczko-Adamczyk, M. Schiemangk, T. Schuldt, A. Peters, T. Könemann, H. Müntinga, C. Lämmerzahl, H. Dittus, T. Steinmetz, T. W. Hänsch, and J. Reichel, “Bose-einstein condensation in microgravity,” *Science* **328**, 1540 (2010).
- [22] G. Condon, M. Rabault, B. Barrett, L. Chichet, R. Arguel, H. Eneriz-Imaz, D. Naik, A. Bertoldi, B. Battelier, P. Bouyer, and A. Landragin, “All-optical bose-einstein condensates in microgravity,” *Phys. Rev. Lett.* **123**, 240402 (2019).
- [23] N. Lundblad, R. A. Carollo, C. Lannert, M. J. Gold, X. Jiang, D. Paseltiner, N. Sergay, and D. C. Aveline, “Shell potentials for microgravity bose-einstein condensates,” *npj Microgravity* **5**, 30 (2019).
- [24] Kai Frye, Sven Abend, Wolfgang Bartosch, Ahmad Bawamia, Dennis Becker, Holger Blume, Claus Braxmaier, Sheng-Wey Chiow, Maxim A. Efremov, Wolfgang Ertmer, Peter Fierlinger, Naceur Gaaloul, Jens Grosse, Christoph Grzeschik, Ortwin Hellmig, Victoria A. Henderson, Waldemar Herr, Ulf Israelsson, James Kohel, Markus Krutzik, Christian Krbis, Claus Lämmerzahl, Meike List, Daniel Ldtke, Nathan Lundblad, J. Pierre Marburger, Matthias Meister, Moritz Mihm, Holger Müller, Hauke Müntinga, Tim Oberschulte, Alexandros Papakonstantinou, Jaka Perovek, Achim Peters, Arnau Prat, Ernst M. Rasel, Albert Roura, Wolfgang P. Schleich, Christian Schubert, Stephan T. Seidel, Jan Sommer, Christian Spindeldreier, Dan Stamper-Kurn, Benjamin K. Stuhl, Marvin Warner, Thijs Wendrich, Andr

- Wenzlawski, Andreas Wicht, Patrick Windpassinger, Nan Yu, and Lisa Wrner, “The bose-einstein condensate and cold atom laboratory,” (2019), [arXiv:1912.04849](https://arxiv.org/abs/1912.04849).
- [25] Alexander L. Fetter, “Rotating trapped bose-einstein condensates,” *Rev. Mod. Phys.* **81**, 647 (2009).
- [26] J M Kosterlitz and D J Thouless, “Ordering, metastability and phase transitions in two-dimensional systems,” *Journal of Physics C: Solid State Physics* **6**, 1181 (1973).
- [27] Arturo Tozzi and David Papo, “Projective mechanisms subtending real world phenomena wipe away cause effect relationships,” *Progress in Biophysics and Molecular Biology* **151**, 1 (2020).
- [28] H. Lamb, [Hydrodynamics](#), Dover Books on Physics (Dover publications, 1945).
- [29] Burt A. Ovrut and Steven Thomas, “Theory of vortices and monopoles on a sphere,” *Phys. Rev. D* **43**, 1314 (1991).
- [30] Nils-Eric Guenther, Pietro Massignan, and Alexander L. Fetter, “Superfluid vortex dynamics on a torus and other toroidal surfaces of revolution,” *Phys. Rev. A* **101**, 053606 (2020).
- [31] A. L. Fetter and R. J. Donnelly, “On the equivalence of vortices and current filaments,” *The Physics of Fluids* **9**, 619 (1966).
- [32] V Vitelli and D. R. Nelson, “Nematic textures in spherical shells,” *Phys. Rev. E* **74**, 021711 (2006).
- [33] Ari M. Turner, Vincenzo Vitelli, and David R. Nelson, “Vortices on curved surfaces,” *Rev. Mod. Phys.* **82**, 1301 (2010).
- [34] Luca Calderaro, Alexander L. Fetter, Pietro Massignan, and Peter Wittek, “Vortex dynamics in coherently coupled bose-einstein condensates,” *Phys. Rev. A* **95**, 023605 (2017).
- [35] Alexander L. Fetter, “Vortices in an imperfect bose gas. iv. translational velocity,” *Phys. Rev.* **151**, 100 (1966).
- [36] C. J. Pethick and H. Smith, [BoseEinstein Condensation in Dilute Gases](#), 2nd ed. (Cambridge University Press).
- [37] P. Rosenbusch, V. Bretin, and J. Dalibard, “Dynamics of a single vortex line in a bose-einstein condensate,” *Phys. Rev. Lett.* **89**, 200403 (2002).
- [38] Amandine Aftalion and Tristan Riviere, “Vortex energy and vortex bending for a rotating bose-einstein condensate,” *Phys. Rev. A* **64**, 043611 (2001).
- [39] Amandine Aftalion and Ionut Danaila, “Three-dimensional vortex configurations in a rotating bose-einstein condensate,” *Phys. Rev. A* **68**, 023603 (2003).
- [40] M. Modugno, L. Pricoupenko, and Y. Castin, “Bose-einstein condensates with a bent vortex in rotating traps,” *Eur. Phys. J. D* **22**, 235 (2003).
- [41] M. L. Chiofalo, S. Succi, and M. P. Tosi, “Ground state of trapped interacting bose-einstein condensates by an explicit imaginary-time algorithm,” *Phys. Rev. E* **62**, 7438 (2000).
- [42] P. G. Kevrekidis, Wenlong Wang, R. Carretero-González, D. J. Frantzeskakis, and Shuangquan Xie, “Vortex precession dynamics in general radially symmetric potential traps in two-dimensional atomic bose-einstein condensates,” *Phys. Rev. A* **96**, 043612 (2017).
- [43] Alexander L. Fetter, “Low-lying superfluid states in a rotating annulus,” *Phys. Rev.* **153**, 285 (1967).
- [44] Nils-Eric Guenther, Pietro Massignan, and Alexander L. Fetter, “Quantized superfluid vortex dynamics on cylindrical surfaces and planar annuli,” *Phys. Rev. A* **96**, 063608 (2017).
- [45] Anatoly A. Svidzinsky and Alexander L. Fetter, “Dynamics of a vortex in a trapped bose-einstein condensate,” *Phys. Rev. A* **62**, 063617 (2000).
- [46] N.R. Cooper, “Rapidly rotating atomic gases,” *Advances in Physics* **57**, 539 (2008).
- [47] David L. Feder, Charles W. Clark, and Barry I. Schneider, “Nucleation of vortex arrays in rotating anisotropic bose-einstein condensates,” *Phys. Rev. A* **61**, 011601 (1999).
- [48] Yongyong Cai, Yongjun Yuan, Matthias Rosenkranz, Han Pu, and Weizhu Bao, “Vortex patterns and the critical rotational frequency in rotating dipolar bose-einstein condensates,” *Phys. Rev. A* **98**, 023610 (2018).
- [49] Amandine Aftalion, Xavier Blanc, and Jean Dalibard, “Vortex patterns in a fast rotating bose-einstein condensate,” *Phys. Rev. A* **71**, 023611 (2005).
- [50] Kenichi Kasamatsu, Makoto Tsubota, and Masahito Ueda, “Giant hole and circular superflow in a fast rotating bose-einstein condensate,” *Phys. Rev. A* **66**, 053606 (2002).